ОБЪЕДИНЕННЫЙ
ИНСТИТУТ
ЯДЕРНЫХ
ИССЛЕДОВАНИЙ

Дубна

D13-2017-28

I. Chirikov-Zorin

NEW METHOD FOR DETERMINING AVALANCHE BREAKDOWN VOLTAGE OF SILICON PHOTOMULTIPLIERS

Presented at the International Conference "Instrumentation for Colliding Beam Physics" (INSTR17), 27 February – 3 March 2017, Novosibirsk, Russia

In modern experimental physics, development of new devices shows a clear trend to replace traditional optical detectors by silicon photomultipliers (Si PMs) — a new generation of photodetectors. Si PMs are micropixel silicon avalanche photodiodes operating in the so-called Geiger mode at a bias voltage higher than the breakdown voltage. Therefore, Si PMs have a high internal amplification rate $\sim 10^6$ at room temperature and can detect weak light fluxes at a level of individual photons counts.

The internal gain in the photodiode can be obtained, in principle, by creating a strong electric field in the depleted region of the p–n junction, and free charge carriers accelerated in this field could produce impact ionization of the p–n junction and develop the avalanche multiplication process. The dependence of the gain G on the reverse bias voltage V_b of the avalanche photodiode (APD) and different regions of the electric discharge by analogy with the operating modes of the gas counter of nuclear radiation are schematically shown in Fig. 1.

The multiplication process of free carriers in the p–n junction is characterized by a k-factor equal to the ratio of the impact ionization coefficients of holes and electrons ($k = \beta/\alpha$). For silicon, $\alpha > \beta$ for any values of the electric field strength [1, 2]. In the proportional region (i.e., when the output signal is proportional to the intensity of the detected light) avalanche multiplication is mainly due to electrons ($k \ll 1$) and therefore the avalanche is quenched. The

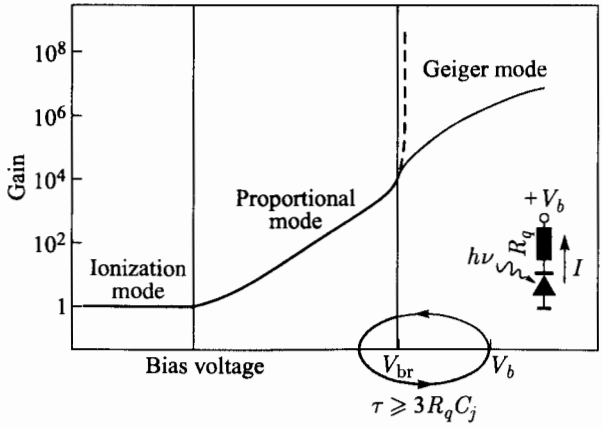

Fig. 1. The schematic representation of the gain versus the reverse bias voltage for an avalanche photodiode

gain of the avalanche photodiode in the proportional mode $G_e \geqslant \exp(\alpha W)$, where W is the width of the avalanche multiplication zone and reaches 10^4 at room temperature [3].

With increasing V_b the electric field strength in the depletion region of the p–n junction grows, which leads to an increase in the impact ionization coefficients of electrons and holes, and k-factor [2]. The avalanche multiplication at a bias voltage higher than a certain threshold value, so-called breakdown $V_{\rm br}$, is due to both electrons and holes ($k \to 1$). At high electric fields ($E \geqslant 5 \cdot 10^5$ V/cm), impact ionization of the p–n junction by holes gives rise to positive internal feedback and, as a consequence, to development of self-sustaining electron–hole avalanche and thermal breakdown of the photodiode p–n junction [4]. At the bias voltage $> V_{\rm br}$, production of one electron–hole pair in the avalanche multiplication region of the p–n junction is enough to initiate a self-sustaining discharge with a formal gain $G \to \infty$. The probability of triggering the avalanche breakdown by an electron or a hole is given by $P_{\rm pair} = P_e + P_h - P_e P_h$, where P_e and P_h are the electrons and holes triggering probabilities. It is important to note that when $V_b = V_{\rm br}$, the triggering probability is $P_e = P_h = 0$.

The discharge can be interrupted by a quenching resistor R_q connected in the bias circuit in series with a photodiode (Fig. 1), which creates a negative external feedback. To quench the discharge, it is necessary to reduce on the p–n junction to voltage $V_{\rm br}$, i.e., the voltage drop across the resistor during the discharge should be equal to or larger than the so-called overvoltage $\Delta V = V_b - V_{\rm br}$. Thus, for quenching the discharge the condition $R_q I \geqslant V_b - V_{\rm br}$ should be fulfilled. The electron–hole avalanche stops when $V_b = V_{\rm br}$, but the voltage across the photodiode continues to decrease as a result of draining of the accumulated charge carriers from the p–n junction to the base regions of the APD.

The time of recovery of the p–n junction potential to its original condition after the avalanche discharge is $\tau \geqslant 3 R_q C_j$ in accordance with the exponential law of the recharging of the p–n junction capacitance C_j through the quenching resistor R_q. With increasing bias voltage, the recovery time significantly increases as a result of partial discharge of C_j due to the increase in the dark current, and others [5].

Thus, the APD operation at a bias voltage higher than the breakdown voltage with negative feedback made via the resistor R_q in the bias circuit in series with the photodiode is called the Geiger mode by analogy with the gas-discharge Geiger–Muller counter. Due to the linear element R_q connected in the bias circuit, the gain in the Geiger mode is a linear function of the overvoltage $G_{eh} \sim C_j(V_b - V_{\rm br})$.

The silicon photomultiplier is a matrix of identical small p–n junctions (pixels) with quenching resistors connected in parallel on the surface of the common silicon substrate. The typical pixel density is 10^2–10^4 mm^{-2} with a pitch of 10–100 μm.

The pixels are independent photon microcounters working in the digital (Geiger) "yes/no" mode. They generate a standard signal when detecting a single photon, but at the detection flashes of light, when a lot of pixels are simultaneously fired, the output signal on the total load is a sum of standard signals. Thus, the Si PM is in general an analog device capable of measuring the intensity of light with a dynamic range corresponding to the total number of pixels.

The main characteristics of the Si PM (gain, detection efficiency, and others) are determined by the overvoltage $\Delta V = V_b - V_{\rm br}$. Therefore, the avalanche breakdown voltage $V_{\rm br}$ is an important parameter, the determination of which is necessary for detailed studies and application of the Si PM. The spread of $V_{\rm br}$ allows estimating the influence of different technological factors and processes in the development and production of the Si PM.

Note that $V_{\rm br}$ increases with temperature. The temperature coefficient of the avalanche breakdown voltage $V_{\rm br}(T)$ is also an important parameter of Si PM.

There are several methods for determining the breakdown voltage of the Si PM [6–16], which are based on different assumptions and models and therefore have limited accuracy. The new physically motivated precision method for determining $V_{\rm br}$ is based on measurements of the relative Si PM detection efficiency.

The photon detection efficiency (PDE) is the product of the geometrical factor ε (ratio of sensitive area to total surface of Si PM), pixel quantum efficiency QE, and probability $P_{\rm tr}$ for triggering avalanche breakdown by the produced free charge carriers:

$$PDE = \varepsilon QE(\lambda) P_{\rm tr}(\lambda, T, \Delta V).$$

The quantum efficiency of the pixel is determined by the probability for production of the charge carriers in the sensitive volume and significantly depends on the wavelength λ of the detected light:

$$QE(\lambda) = [1 - r][\exp(-L_{\rm ep}/\lambda_{\rm ep}(\lambda))][\exp(-L_{\rm SiO_2}/\lambda_{\rm SiO_2}(\lambda))] \times \\ \times [1 - \exp(-L_{\rm Si}/\lambda_{\rm Si}(\lambda))],$$

where r is the reflection coefficient from the pixel surface, $L_{\rm ep}$ and $L_{\rm SiO_2}$ are the thicknesses of the epoxy resin and silicon oxide layers used as protective coatings, $\lambda_{\rm ep}(\lambda)$ and $\lambda_{\rm SiO_2}(\lambda)$ are the light absorption lengths in the coatings, $L_{\rm Si} = W_n + W + W_p$ is the thickness of the sensitive layer (Fig. 2), and $\lambda_{\rm Si}(\lambda)$ is the light absorption length in silicon.

The avalanche breakdown triggering probability depends on the overvoltage and on the position where the primary electron–hole pair is produced in the sensitive layer of the pixel. Three photogeneration zones of primary electron–hole pairs W_n, W, W_p and their typical thickness [17] are shown in Fig. 2. The triggering probability of the electron–hole pair in the avalanche multiplication

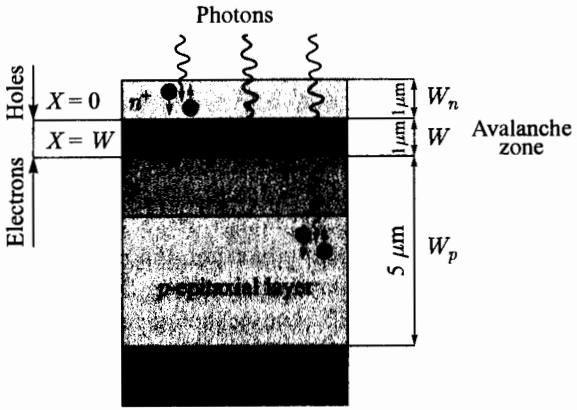

Fig. 2. A simplified schematic view of the pixel structure on the p-substrate

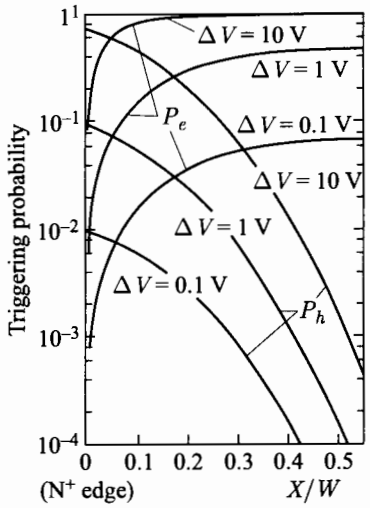

Fig. 3. The triggering probabilities $P_e(x, \Delta V)$ and $P_h(x, \Delta V)$ as a function of the positions of the carriers generated in the avalanche multiplication zone with a width W at several overvoltage values ΔV [18]. Coordinates of the zone boundaries $X = 0$ and $X = W$ are shown in Fig. 2

zone W is given by

$$P_{\text{pair}}(x, \Delta V) = P_e(x, \Delta V) + P_h(x, \Delta V) - P_e(x, \Delta V)P_h(x, \Delta V),$$

where $P_e(x, \Delta V)$ and $P_h(x, \Delta V)$ are the triggering probabilities for electrons and for holes generated at the point with the coordinate x at overvoltage ΔV. Figure 3 shows the dependence of $P_e(x, \Delta V)$ and $P_h(x, \Delta V)$ on the coordinates of the generation of charge carriers in the avalanche multiplication zone calculated by W. G. Oldham et al. [18].

Electrons and holes produced in the zone W_p drift in the electric field in opposite directions, holes to the p-base and electrons to the avalanche multiplication zone W, and thus the latter can trigger an avalanche breakdown. On the contrary, if the photons are absorbed in zone W_n, an avalanche can be triggered only by holes. The avalanche triggering probability of electrons and holes produced outside multiplication zone W was calculated and verified experimentally by P. Antognetti, W. G. Oldham (Fig. 4) [19]. The triggering probability of holes is much lower than that of electrons due to the difference between their impact ionization coefficients ($\alpha > \beta$).

As can be seen in Fig. 4, the triggering probabilities of electrons and holes injected into the avalanche multiplication zone of the p–n junction are linear functions of overvoltage at its low values (1–2 V). The PDE is proportional to the triggering probability; therefore, it is also a linear function of the overvoltage and consequently of the bias voltage V_c. Extrapolation of the function $PDE = PDE(V_c)$ or relative $PDE_{\text{rel}} = PDE_{\text{rel}}(V_c)$ to zero values determines the Si PM avalanche breakdown voltage.

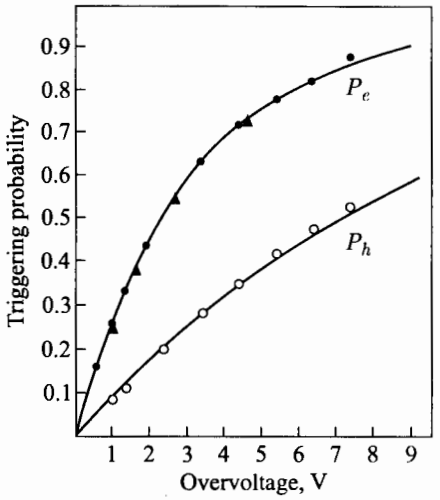

Fig. 4. The avalanche triggering probabilities for electrons P_e and for holes P_h as a function of the overvoltage ΔV [19]

Electrons or holes can be injected into the W avalanche multiplication zone using short-wave or long-wave light. If the Si PM is illuminated by short-wave light with $\lambda = 400$ nm, it is almost completely absorbed ($> 99\%$) in the layer W_n, and holes will drift into the zone W. If the Si PM is illuminated by long-wavelength light with $\lambda = 1000$ nm, which is weakly absorbed in thin W_n and W layers ($\approx 1\%$), it is mainly electrons that will drift from the layer W_p into the avalanche multiplication zone.

To illustrate the method, we determine the avalanche breakdown voltage for the Si PMs of two types, SSPM-050701GR-TO18 and S60 [20]. Their PDE is measured by the method of low-intensity light flashes (~ 10 photons) method [21, 22], when the probability for production of free charge carriers in the sensitive layer of Si PM is low.

A typical LED charge spectrum of the Si PM for low-intensity light pulses is shown in Fig. 5. In accordance with the Poisson distribution $P(n; \mu) = \mu^n \exp(-\mu)/n!$, the average number of photogenerated pairs that triggered avalanche breakdown pixels of the Si PM is

$$\mu = -\ln P(0; \mu),$$

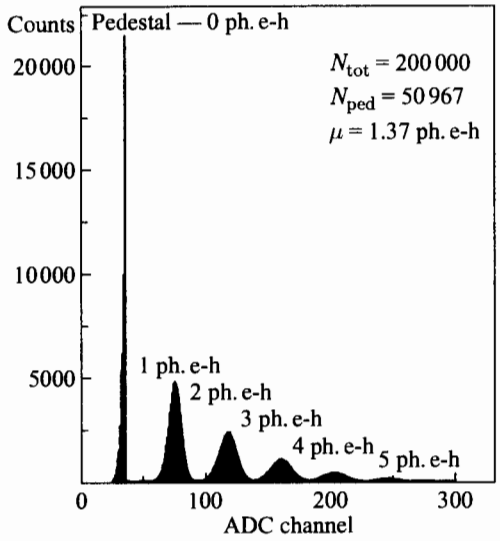

Fig. 5. The S60 Si PM pulse height spectrum for low-intensity light flashes with the mean number of photogenerated electron–hole pairs $\mu = 1.37$ ph. e–h

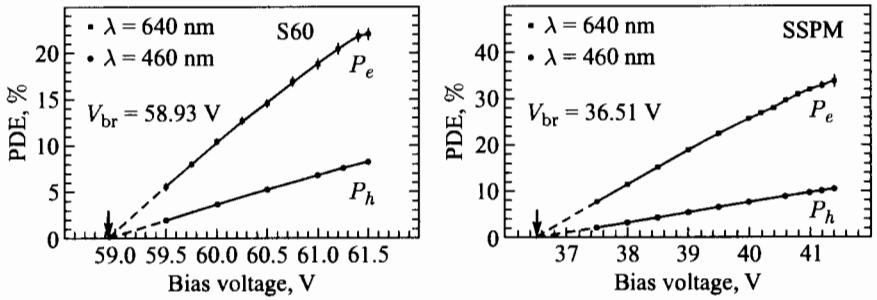

Fig. 6. The photon detection efficiency as a function of the overvoltage for different wavelengths of light for the S60 and SSPM-050701GR-TO18 Si PMs based on p-substrate

where $P(0;\mu) = N_{ped}/N_{tot}$ is the probability of non-generation of a signal from Si PM, N_{ped} is the number of events in the pedestal and N_{tot} is the total number of events in the spectrum. The photon detection efficiency was determined from the expression

$$PDE = -\ln(N_{ped}/N_{tot})/N_{ph},$$

where N_{ph} is the average number of photons incident on the Si PM. The average number of photons was estimated by the H6780-04 photosensor (Hamamatsu) with the known quantum efficiency using the low-intensity light flash method.

The PDE measurement was performed using red ($\lambda \approx 640$ nm) and blue ($\lambda \approx 460$ nm) light, when mainly one type of free charge carriers, electrons or holes, are injected into the avalanche multiplication region. The linear extrapolation of the initial part of $PDE = PDE(V_c)$ dependence to zero values determines the Si PM avalanche breakdown voltage (Fig. 6). The values of breakdown voltage obtained for different wavelengths of light coincide with high accuracy $\sim 10^{-3}$ V, which confirms the reliability of the proposed method.

REFERENCES

1. S. M. Sze, Physics of semiconductor devices. A Wiley-Interscience Publication, New York, 1981.
2. Y. Musienko et al., A simple model of EG&G reverse reach-through APDs. Nucl. Instr. Meth. A 442 (2000) 179.
3. R. Farrell et al., Radiation detection performance of very high gain avalanche photodiodes. Nucl. Instr. Meth. A 353 (1994) 176.
4. I. Tapan et al., Avalanche photodiodes as proportional particle detectors. Nucl. Instr. Meth. A 388 (1997) 79.
5. L. Gruber et al., Recovery time measurements of silicon photomultipliers using a pulsed laser. arXiv:1510.06906.
6. C. Piemonte et al., IEEE Trans. Nucl. Sci. NS-54 (2007) 236–244.
7. N. Serra et al., IEEE Trans. Nucl. Sci. NS-58 (2011) 1233–1240.
8. Zhengwei Li et al., Nucl. Instr. Meth. A 695 (2012) 222.
9. E. Garutti et al., Characterization and X-ray damage of silicon photomultipliers. PoS(TIPP2014)070.
10. M. Grodzicka et al., Nucl. Instr. Meth. A 783 (2015) 58.
11. Wang Yue et al., Nucl. Instr. Meth. A 787 (2015) 38.
12. C. Heidemann et al., Nucl. Instr. Meth. A 787 (2015) 261.
13. V. Chmill et al., Nucl. Instr. Meth. A 845 (2017) 56.
14. N. Dinu et al., Nucl. Instr. Meth. A 845 (2017) 64.
15. A. Otte et al., Nucl. Instr. Meth. A 846 (2017) 106.
16. F. Nagy et al., Nucl. Instr. Meth. A 849 (2017) 55.
17. P. Buzhan, B. Dolgoshein et al., An advanced study of silicon photomultiplier, ICFA Instrumentation Bulletin, 2001.
18. W. G. Oldham et al., IEEE Trans. Electron. Dev. ED-19 (9) (1972) 1056.
19. P. Antognetti, W. G. Oldham, J. Electronic Materials, 1975, Vol. 4, No. 1.
20. N. Anfimov, I. Chirikov-Zorin et al., Nucl. Instr. Meth. A 572 (2007) 413.
21. E. H. Bellamy et al., Nucl. Instr. Meth. A 339 (1994) 468.
22. I. Chirikov-Zorin et al., Nucl. Instr. Meth. A 456 (2001) 310.

Received on May 18, 2017.